Supporting Information

Unusual Interchromophoric Interactions in β,β′ Directly and Doubly Linked Corrole Dimers; Prohibited Electronic Communication and Abnormal Singlet Ground States

Sung Cho, Jong Min Lim, Satoru Hiroto, Pyosang Kim, Hiroshi Shinokubo, Atsuhiro Osuka,* and Dongho Kim**

(1) Macro-cyclic conjugation pathway of **H_3CM**.

(2) 3D molecular structures of corrole dimers.

(3) Absorption spectra of various corroles in MC.

(4) Absorption spectra of **DH_2CD** and **DZnCD** in MC and toluene.

(5) Absorption spectra and simulated electronic states of **H_3CM** and **SH_3CD.**

(6) Molecular orbital energy levels and shapes of the doubly linked corrole dimers.

(7) Steady-state fluorescence spectra and time-resolved fluorescence decay profiles of corroles.

(8) Time-resolved bleaching recovery profiles of the oxidized corrole dimers.

(9) Vertical NICS scan spectra at constituent corrole units and octagonal cores of **DH_3CD** and **DH_2CD.**

(10) Vertical NICS scan spectra of the optimized **H_2CM** and restricted **H_2CM** from **DH_2CD.**

(11) Transverse NICS scan spectrum of **H_3CM**.

(12) TPA cross-section scan spectrum of **DH_3CD.**

(13) Difference of the bond length alternation between **DH_3CD** and **DH_2CD.**

(14) Transition symmetries of **DH_2CD** with D_{2h} symmetry.

(15) Simulated electronic states of **H_3CM**, **DH_3CD**, **DH_2CD**, and **DZnCD**.

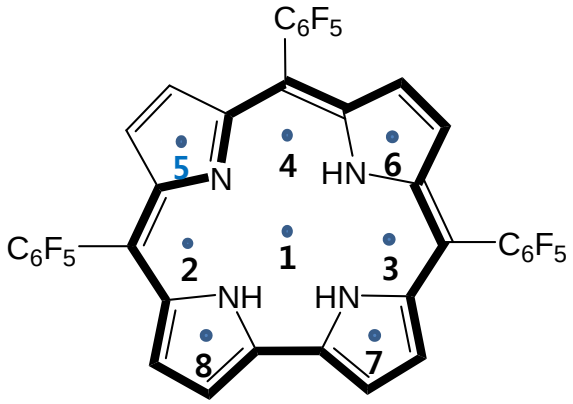

Position	NICS / ppm
1	-12.9
2	-15.5
3	-17.9
4	-16.3
5	-4.97
6	-14.0
7	-17.8
8	-14.2

Figure S1. Macro-cyclic conjugation pathway of **H_3CM** and calculated NICS values at several centroids.

1) Aihara, J.-I. *J. Phys. Chem. A* **2008,** *112,* 5305.

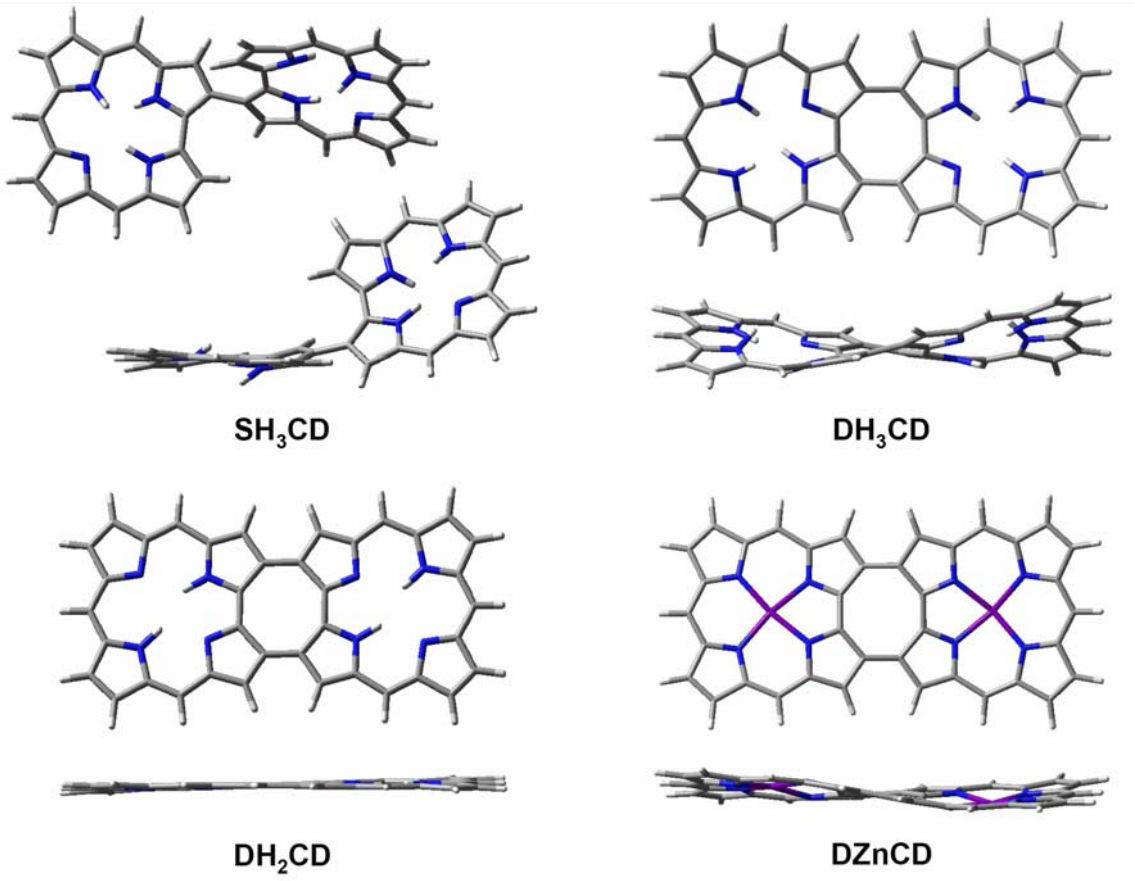

Figure S2. 3D molecular structures of corrole dimers (C_6F_5 substituents are not shown).

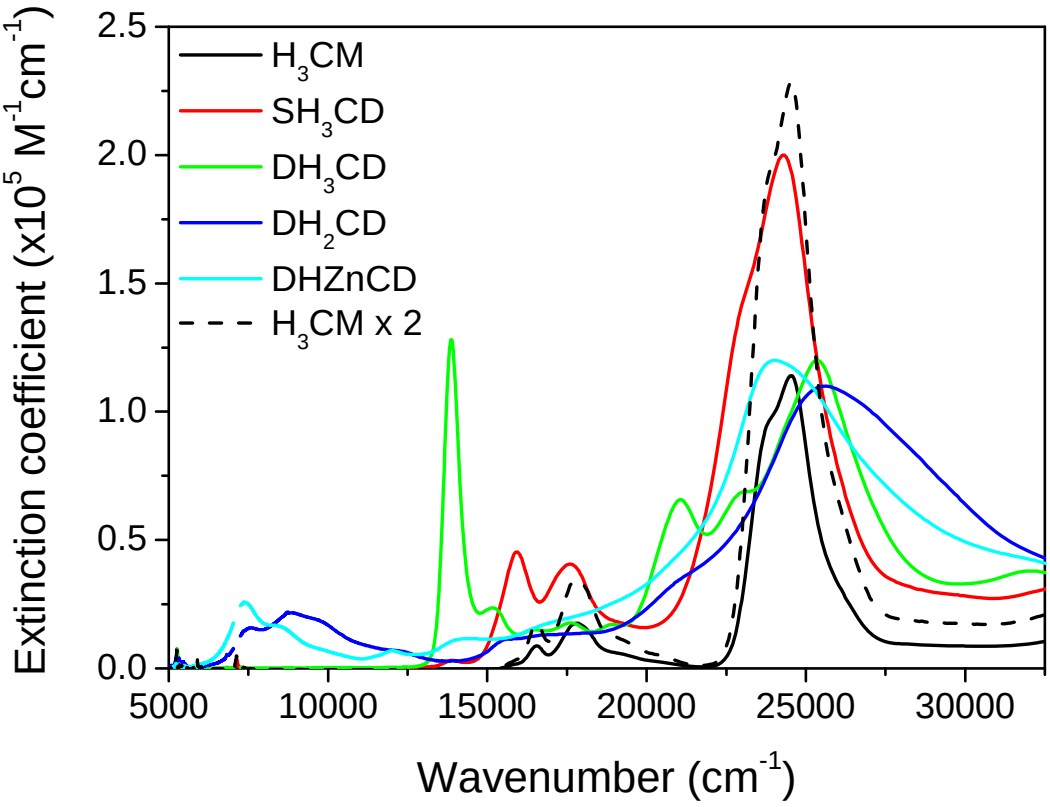

Figure S3. Steady-state absorption spectra of various corroles in CH_2Cl_2.

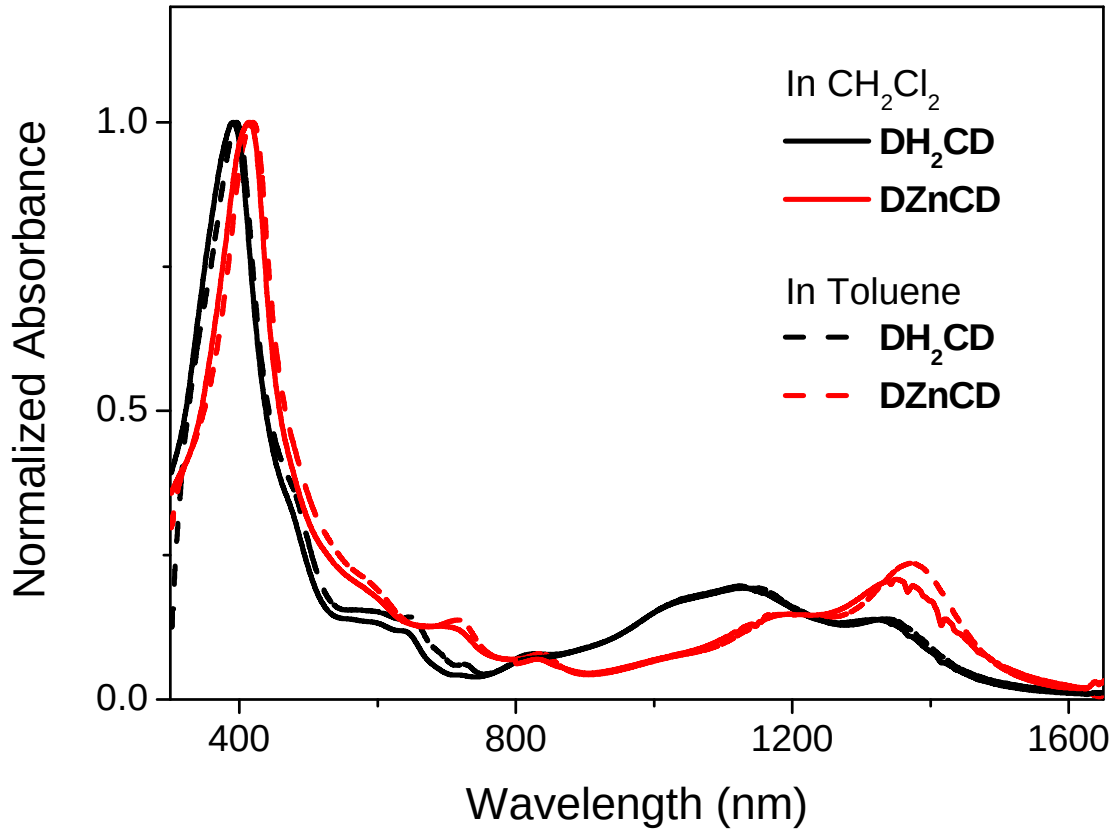

Figure S4. Steady-state absorption spectra of **DH_2CD** and **DZnCD** in CH_2Cl_2 and toluene.

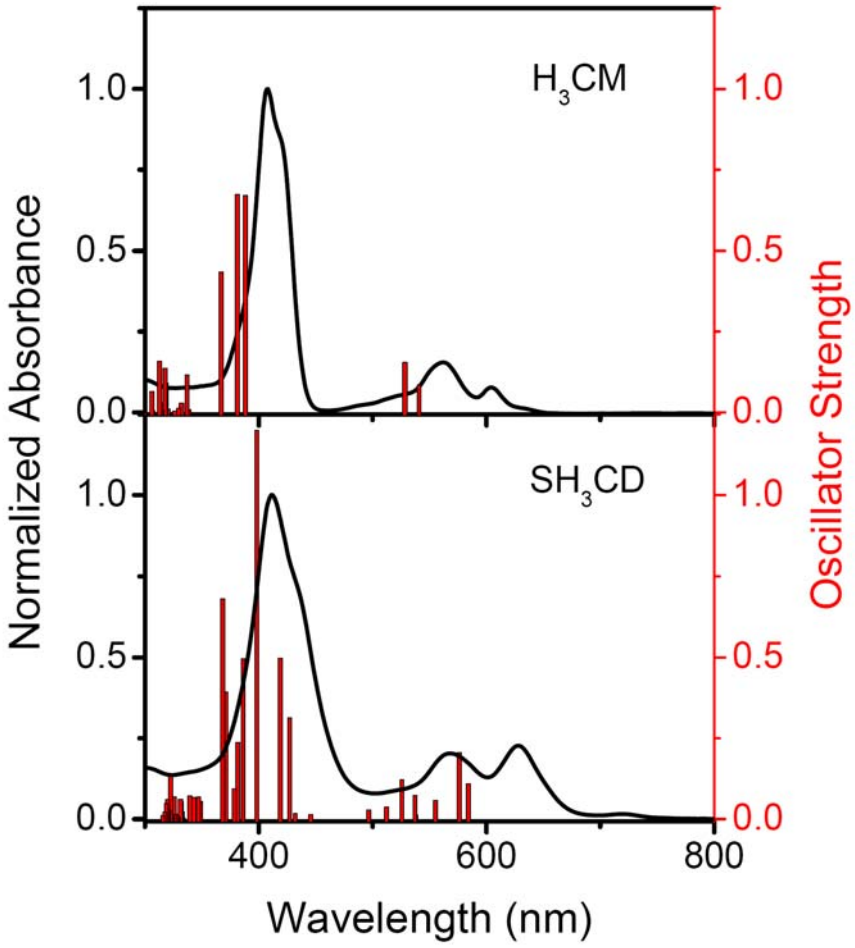

Figure S5. Steady-state absorption spectra and simulated singlet electronic states of **H3CM** and **SH3CD**.

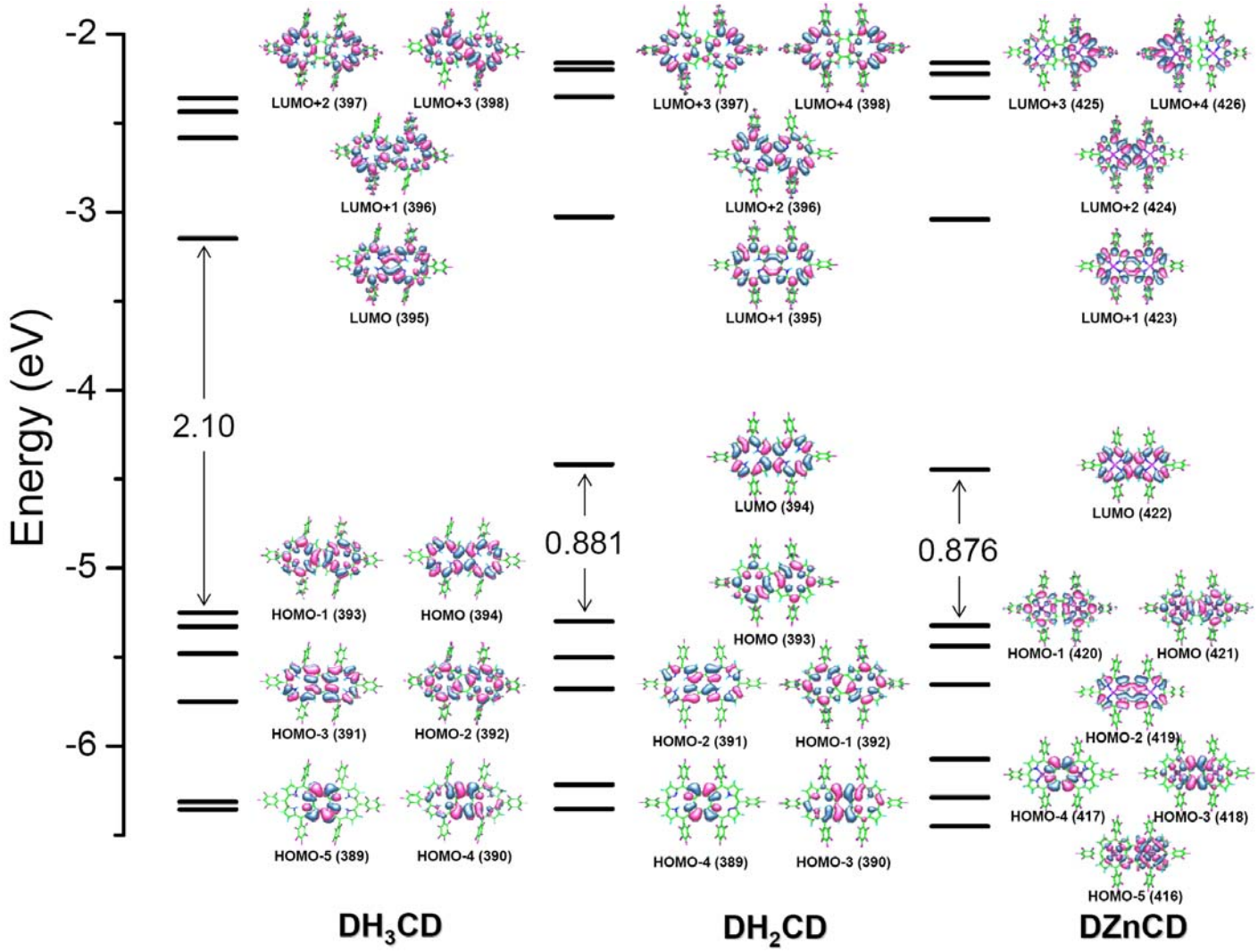

Figure S6. Molecular orbital energy levels and shapes of **DH₃CM**, **DH₂CD**, and **DZnCD**.

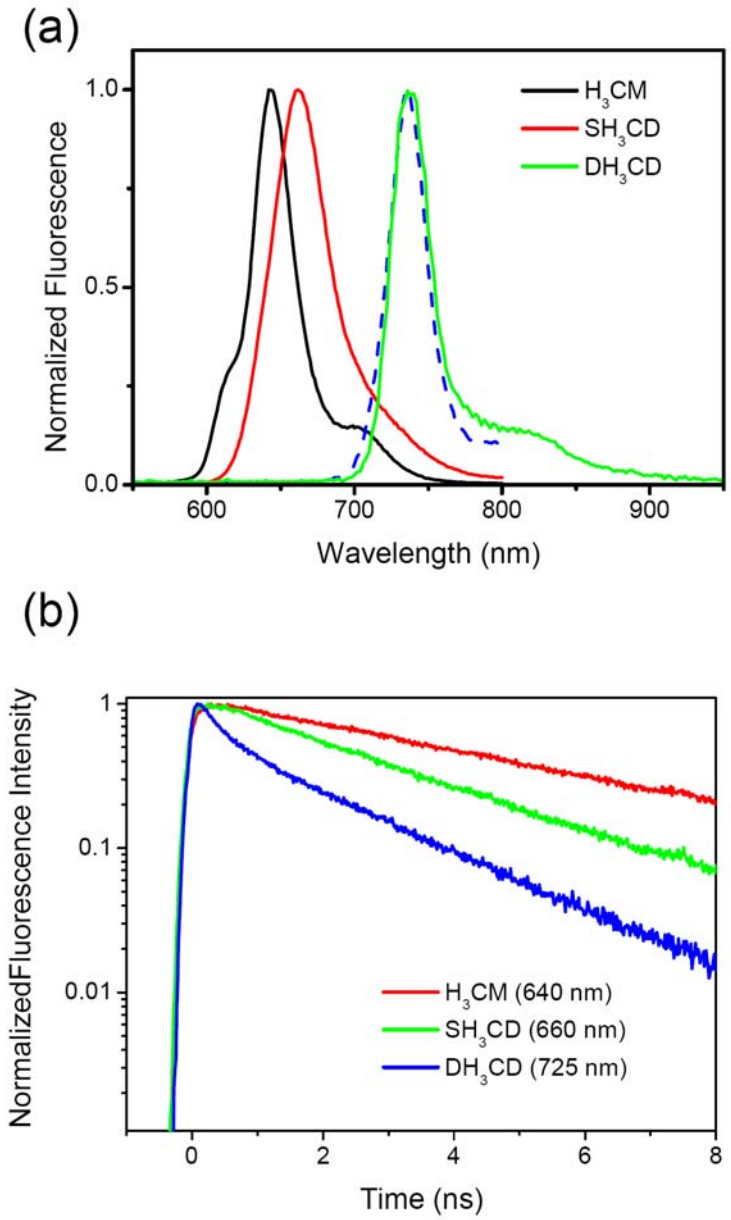

Figure S7. Steady-state fluorescence spectra and time-resolved fluorescence decay profiles of **H3CM**, **SH3CD**, and **DH3CD**.

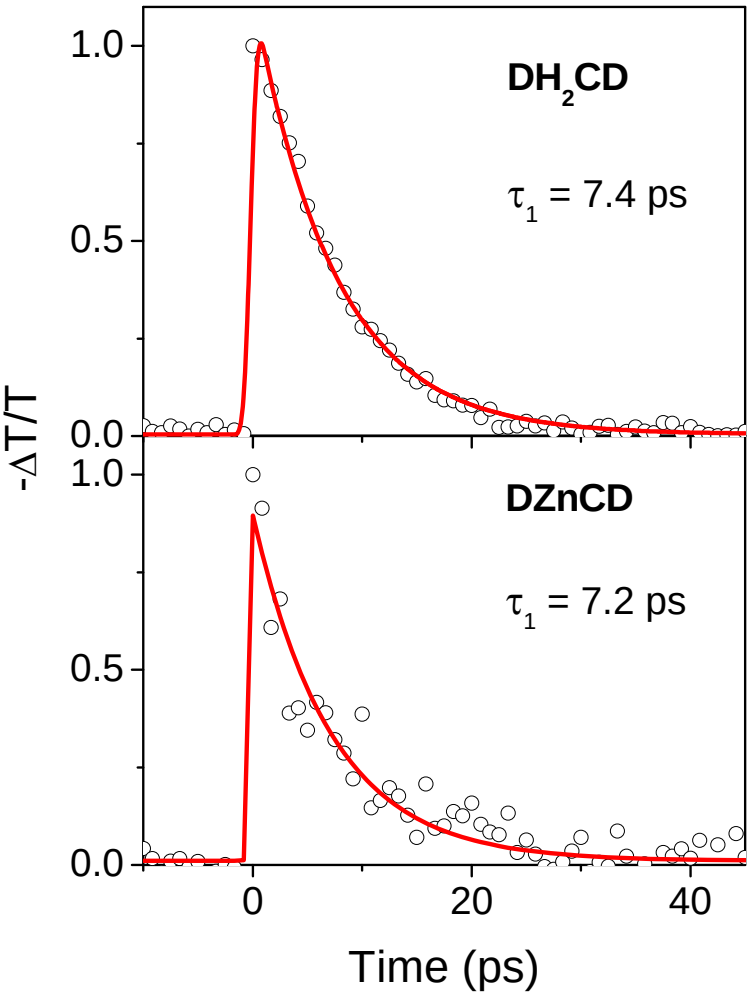

Figure S8. Time-resolved bleaching recovery profiles of **DH₂CD** and **DZnCD** (pump: 400 nm, probe: 550 nm).

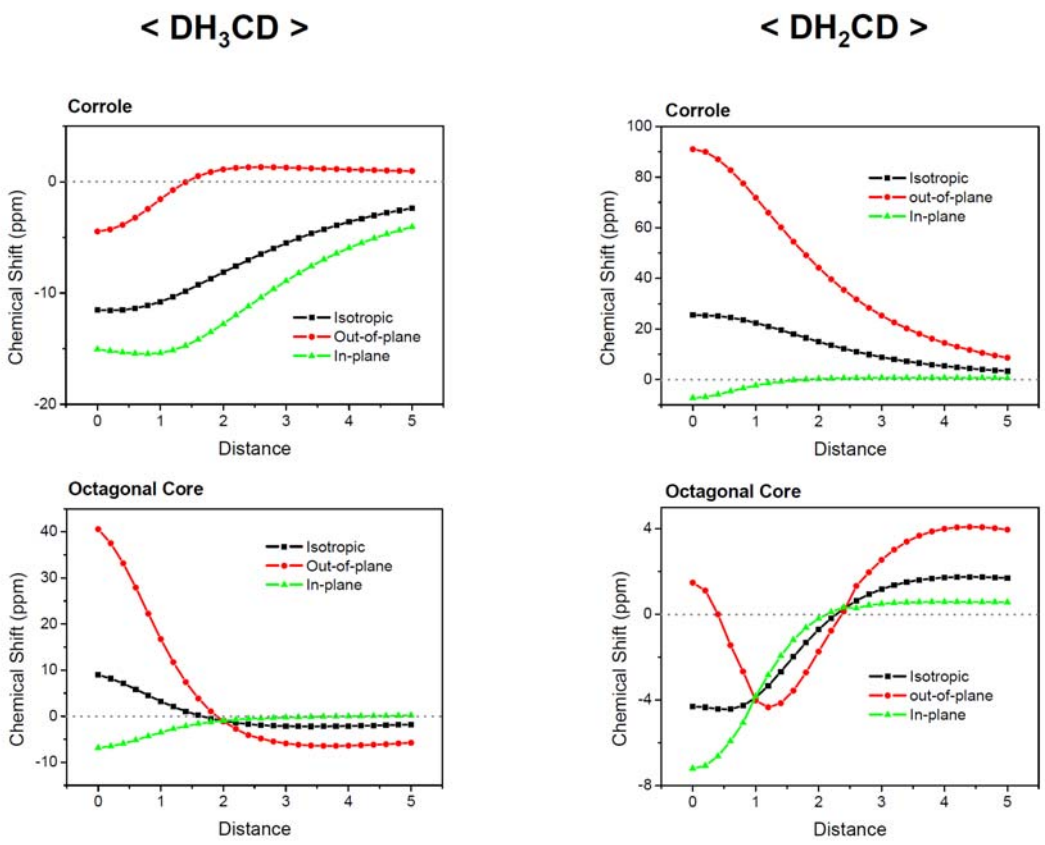

Figure S9. Vertical NICS scan spectra at constituent corrole units and octagonal cores of **DH₃CD** and **DH₂CD**.

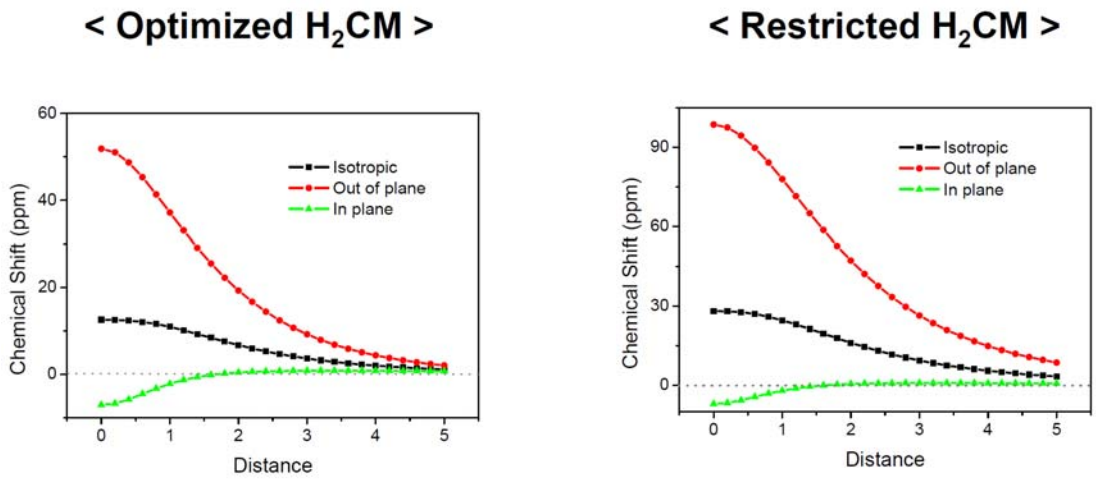

Figure S10. Vertical NICS scan spectra of the optimized **H₂CM** and restricted **H₂CM** from **DH₂CD**.

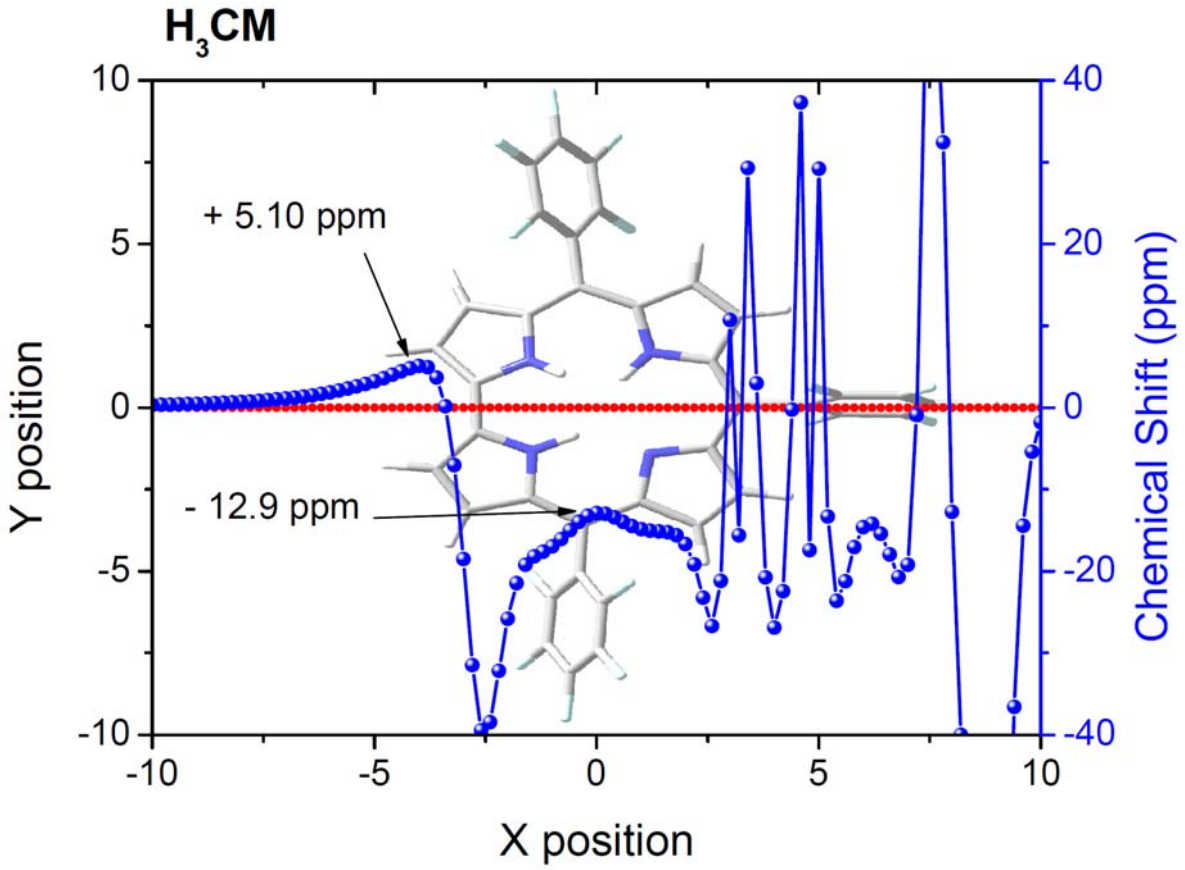

Figure S11. Transverse NICS scan spectrum of **H_3CM** (the red and blue circles are geometrical positions and corresponding NICS values, respectively).

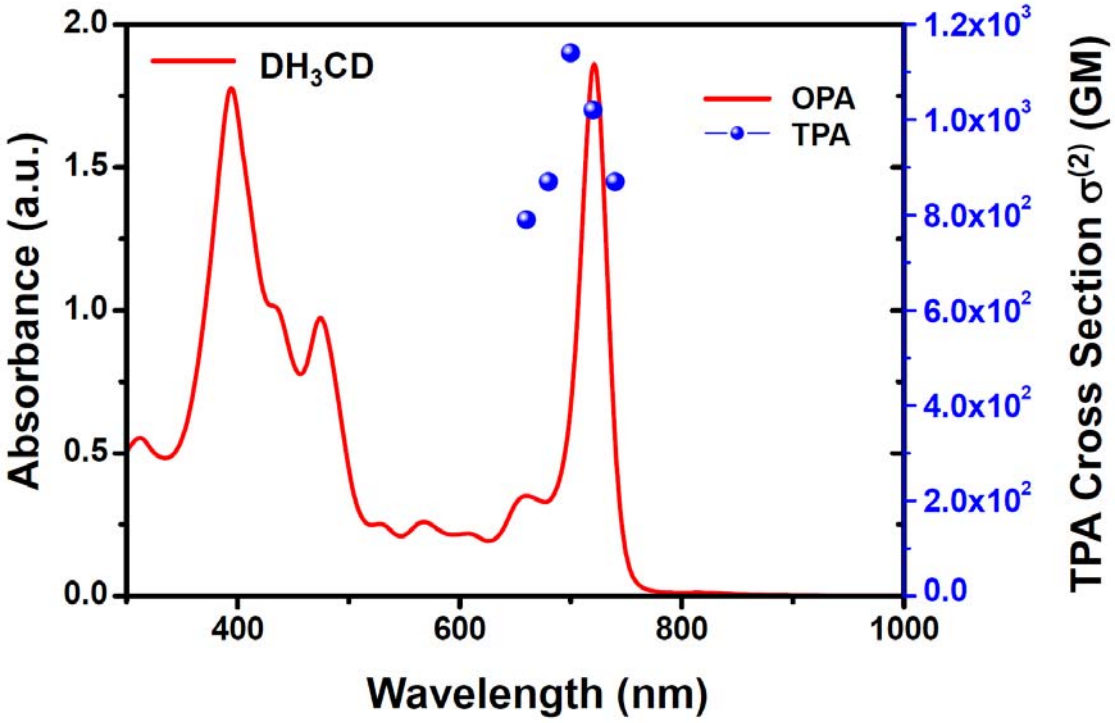

Figure S12. TPA cross-section scan spectrum of **DH₃CD**.

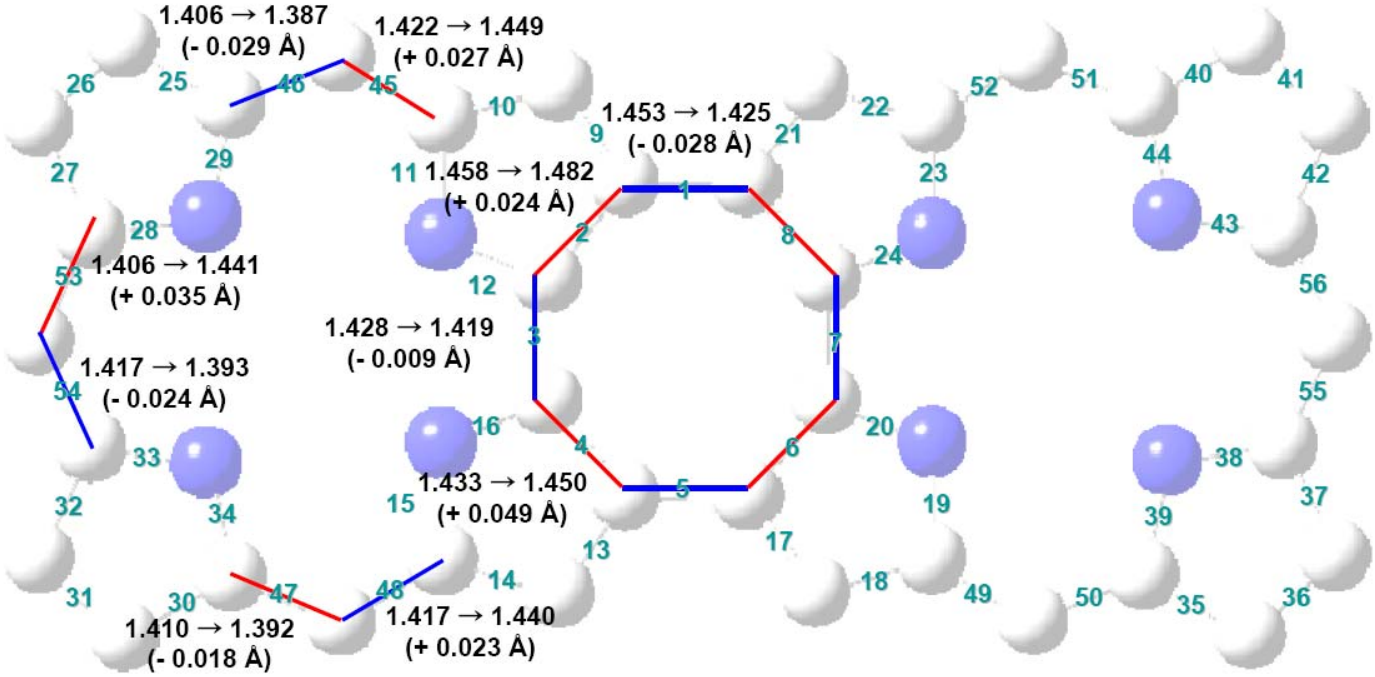

Figure S13. Difference of the bond length alternation between **DH$_3$CD** and **DH$_2$CD**.

Table S1. Transition symmetries of **DH_2CD** with D_{2h} symmetry.

D_{2h}	E	$C_2(z)$	C2(y)	C2(x)	i	s(xy)	s(xz)	s(yz)		
Ag	1	1	1	1	1	1	1	1		
B1g	1	1	-1	-1	1	1	-1	-1		
B2g	1	-1	1	-1	1	-1	1	-1		
B3g	1	-1	-1	1	1	-1	-1	1		
Au	1	1	1	1	-1	-1	-1	1		
B1u	1	1	-1	-1	-1	-1	1	1		
B2u	1	-1	1	-1	-1	1	-1	1		
B3u	1	-1	-1	1	-1	1	1	-1		
LUMO	1	1	1	1	-1	-1	-1	-1	Au	
HOMO	1	-1	1	-1	1	-1	1	-1	B2g	
HOMO-LUMO	1	-1	1	-1	-1	1	-1	1	B2u (y)	optically allowed but energetically forbidden
HOMO-1	1	1	-1	-1	-1	-1	1	1	B1u	
HOMO-1-LUMO	1	1	-1	-1	1	1	-1	-1	B1g	optically forbidden
HOMO-2	1	-1	-1	1	1	-1	-1	1	B3g	
HOMO-2-LUMO	1	-1	-1	1	-1	1	1	-1	B3u (x)	optically allowed

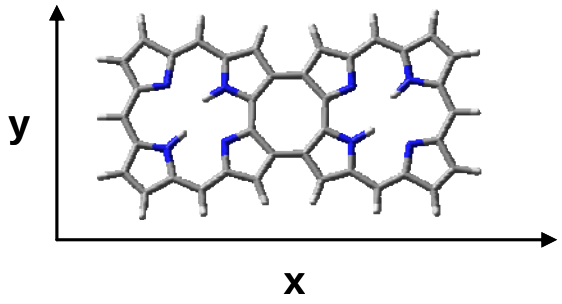

Table S2. Simulated singlet excited states of **H_3CM**, **DH_3CD**, **DH_2CD**, and **DZnCD** by using TD-DFT calculations.

H_3CM

Excited State 1: Singlet-A	2.2903 eV 541.35 nm f=0.0945	
197 →199	.41104	33.8 %
197 → 200	-.23036	10.6 %
198 → 199	.37625	28.3 %
198 → 200	.35514	25.2 %

Excited State 2: Singlet-A	2.3363 eV 530.69 nm f=0.1368	
197 → 199	-.34800	24.2 %
197 → 200	-.27274	14.9 %
198 → 199	.43550	37.9 %
198 → 200	-.29654	17.6 %

Excited State 3: Singlet-A	3.2394 eV 382.74 nm f=0.7637	
196 → 199	-.14441	4.2 %
196 → 200	-.18695	7.0 %
197 → 199	-.26658	14.2 %
197 → 200	.28272	16.0 %
198 → 199	.11001	2.4 %
198 → 200	.35733	25.5 %

Excited State 4: Singlet-A	3.2979 eV 375.95 nm f=0.7512	
196 → 199	-.32576	21.2 %
197 → 199	.17769	6.3 %
197 → 200	.35786	25.6 %
198 → 199	.14851	4.4 %
198 → 200	-.26747	14.3 %
198 → 201	-.12723	3.2 %

Excited State 5: Singlet-A	3.4176 eV 362.78 nm f=0.4547	
196 → 199	.57585	66.3 %
197 → 200	.27555	15.2 %
198 → 199	.11185	2.5 %

DH_3CD

Excited State 1: Singlet-A	1.7529 eV 707.32 nm f=0.0045	
393 → 395	.65779	86.5 %
394 → 396	-.13648	3.7 %
394 → 398	-.10164	2.1 %

Excited State 2: Singlet-A	1.8742 eV 661.53 nm f=0.6346	
392 → 397	-.12232	3.0 %
393 → 398	.12604	3.2 %
394 → 395	.63108	79.7 %

Excited State 3: Singlet-A	1.9992 eV 620.18 nm f=0.0819	
391 → 396	-.11504	2.6 %
392 → 395	.62315	77.7 %
394 → 397	.27400	15.0 %

Excited State 4: Singlet-A	2.2215 eV 558.11 nm f=0.0003	
391 → 395	.62166	77.3 %
392 → 396	.10635	2.3 %
393 → 397	-.16815	5.7 %
394 → 396	.19004	7.2 %
394 → 398	-.12939	3.3 %

Excited State 5: Singlet-A	2.3046 eV 537.97 nm f=0.0088	
390 → 395	.12594	3.2 %
392 → 398	-.24630	12.1 %
393 → 397	.28405	16.1 %
394 → 396	.55926	62.6 %

DH_2CD

Excited State 1: Singlet-A	0.4283 eV 2894.62 nm f=0.0158	
391 → 394	-.27412	15.0 %
393 → 394	.56158	63.1 %

Excited State 2: Singlet-A	0.5585 eV 2219.79 nm f=0.0000	
392 → 394	.66429	88.3 %

Excited State 3: Singlet-A	1.0531 eV 1177.28 nm f=0.4072	
390 → 394	.19149	7.3 %
391 → 394	.51812	53.7 %
393 → 394	.15808	5.0 %

Excited State 4: Singlet-A	1.3551 eV 914.97 nm f=0.0000	
389 → 394	.68046	92.6 %

Excited State 5: Singlet-A	1.3922 eV 890.58 nm f=0.1067	
390 → 394	.62425	77.9 %
391 → 394	-.13480	3.6 %
392 → 395	.14630	4.3 %

Excited State 6: Singlet-A	1.8831 eV 658.40 nm f=0.0001	
388 → 394	-.10250	2.1 %
390 → 395	-.10092	2.0 %
393 → 395	.65718	86.4 %

Excited State 7: Singlet-A	2.2066 eV 561.88 nm f=0.1913	
387 → 394	-.17694	6.3 %
392 → 395	.61176	74.9 %
393 → 396	-.17195	5.9 %

Excited State 8: Singlet-A	2.2462 eV 551.98 nm f=0.0000	
388 → 394	.66873	89.4 %

Excited State 9: Singlet-A	2.2605 eV 548.48 nm f=0.0221	
387 → 394	.64800	84.0 %
392 → 395	.15828	5.0 %

Excited State 10: Singlet-A	2.2832 eV 543.03 nm f=0.0000	
379 → 394	-.21165	9.0 %
391 → 395	.62281	77.6 %
393 → 398	.13275	3.5 %

DZnCD

Excited State 1:	Singlet-A	0.3373 eV	3676.04 nm f=0.0010
421 → 422	.63790		81.4 %

Excited State 2:	Singlet-A	0.4567 eV	2714.73 nm f=0.0001
420 → 422	.66300		87.9 %

Excited State 3:	Singlet-A	1.0732 eV	1155.31 nm f=0.4551
412 → 422	-.10078		2.0 %
419 → 422	.54903		60.3 %

Excited State 4:	Singlet-A	1.1279 eV	1099.27 nm f=0.0166
415 → 422	-.13976		3.9 %
418 → 422	.64708		83.7 %
420 → 423	.10326		2.1 %

Excited State 5:	Singlet-A	1.2433 eV	997.18 nm f=0.0042
417 → 422	.67733		91.8 %

Excited State 6:	Singlet-A	1.3652 eV	908.16 nm f=0.0034
416 → 422	.69220		95.8 %

Excited State 7:	Singlet-A	1.4854 eV	834.70 nm f=0.0032
415 → 422	.67303		90.6 %
418 → 422	.10650		2.3 %

Excited State 8:	Singlet-A	1.8699 eV	663.06 nm f=0.0032
418 → 423	.13560		3.7 %
421 → 423	.65927		86.9 %

Excited State 9:	Singlet-A	2.1173 eV	585.58 nm f=0.1625
405 → 422	.10781		2.3 %
419 → 425	.10779		2.3 %
420 → 423	.63483		80.6 %

Excited State 10:	Singlet-A	2.2457 eV	552.10 nm f=0.0001
407 → 422	-.33782		22.8 %
419 → 423	.57656		66.5 %

Reference 36:
Ohta, S.; Nakano, M.; Kubo, T.; Kamada, K.; Ohta, K.; Kishi, R.; Nakagawa, N.; Champagne, B.; Botek, E.; Takebe, A.; Umezaki, S.-Y.; Nate, M.; Takahashi, H.; Furukawa, S.-I.; Morita, Y.; Nakasuji, K.; Yamaguchi, K. *J. Phys. Chem. A* **2007**, *111*, 3633.